ABSTRACT

Bedrock river incision exerts a primary control on landscape evolution in unglaciated terrain. Quantifying river incision via process rate laws represents a key goal of geomorphic research, but such models often fail to reproduce traits of natural rivers responding to base-level lowering. The Fortymile River flows from eastern Alaska to the Yukon River in Canada, across a tectonically quiescent region with near-uniform precipitation and bedrock erosivity. We exploit these stable boundary conditions to quantify bedrock incision evident in a gravel-capped strath terrace that flanks the lower ~175 km of the river and grades to the minimally incised headwaters. The terrace gravel yields a cosmogenic isochron burial age of 2.44 ± 0.24 Ma, consistent with abandonment triggered by Late Pliocene-Early Pleistocene Yukon River headwater capture. The deeply incised reach forms a linear knickzone where basin relief nearly doubles and inferred bedrock incision rates (~19-110 m/Ma) averaged since ~2.44 Ma increase downstream toward the Fortymile-Yukon River confluence. Background, basin-scale ^{10}Be-based erosion rates for tributaries to the Fortymile River trunk nearly double from the headwaters (~9 mm/ka) to the knickzone (avg. ~16 mm/ka), revealing the pace of ongoing landscape response to knickzone incision over 10^4 y. Our observations allow calibration of a stream power incision model (erosion coefficient K ~ 1.1 $m^{0.2} \times 10^{-6}$) that closely reproduces the knickzone profile and thus implies long-term (10^4-10^6 y) efficacy of a simple stream power bedrock incision law.

Publisher: GSA
Journal: GEOL: Geology
DOI:10.1130/G40203.1

Ongoing bedrock incision of the Fortymile River driven by Plio-Pleistocene Yukon River capture, eastern Alaska and Yukon, Canada

Adrian M. Bender[1*], Richard O. Lease[1], Lee B. Corbett[2], Paul Bierman[2], and Marc W. Caffee[3]

[1]*U.S. Geological Survey, 4210 University Drive, Anchorage, Alaska 99508, USA*

[2]*University of Vermont Department of Geology, 180 Colchester Avenue, Burlington, Vermont 05405, USA*

[3]*Purdue University Department of Physics and Astronomy and Department of Earth, Atmospheric, and Planetary Sciences, 525 Northwestern Avenue, West Lafayette, Indiana 47907, USA*

*E-mail: *abender@usgs.gov*

INTRODUCTION AND SETTING

Bedrock river incision exerts the primary control on landscape evolution in non-glaciated terrain (Whipple et al., 2013). Consequently, characterizing bedrock incision via field-calibrated rate law models represents a first-order goal of quantitative geomorphology. Stream power models that describe bedrock incision rate as a power law function of drainage area and channel slope (e.g., Whipple and Tucker, 1999) occupy a key role in the past several decades of geomorphic research (c.f. Whipple et al., 2013). However, these models achieve limited success in reproducing characteristics of river systems that are adjusting to base level lowering via spatially and temporally transient bedrock incision (Lague, 2014). Some researchers attribute model limitations to overlysimplistic underlying theory that (a) treats rock strength, sediment flux, and erosion mechanics with a single coefficient of erosion (e.g., Sklar and Dietrich, 1998), (b) neglects the role of dynamic channel width adjustment (Lague, 2014), and (c) assumes constant runoff over time and dismisses stochastic flooding (DiBiase and Whipple, 2011). While recent studies explicitly treat these factors with increasingly complex stream power models (Scherler et al., 2017; DiBiase and Whipple, 2011; Lague, 2014), accumulation of empirical data lags the pace of theoretical development. Hence, advancing quantitative understanding of bedrock incision requires field data from transient-state bedrock river systems.

Transient-state bedrock rivers present a host of factors that challenge stream power-based interpretations of incision patterns and rates. For example, relatively few transient rivers record their initial, regional equilibrium channel profiles in the form of graded, dateable strath terraces that enable incision rate calculation and model parameter calibration (Stock and Montgomery, 1999). More often, terraces are deformed along spatial rock uplift gradients so that stream power model calibration requires prior knowledge of both rock uplift and incision rates (Kirby and Whipple, 2001). Downstream changes in rock type can also impart major variations in landscape erosivity that complicate channel response to base-level fall (e.g., Duvall et al., 2004). Furthermore, climatic factors such as spatial precipitation gradients imposed by topography or the erosional imprint of past glaciations can impede straightforward assessment of bedrock river incision patterns and rates.

The Fortymile River flows from eastern Alaska to the Yukon River in Canada (Fig. 1A) across a region where the consistent tectonic, lithologic and climatic conditions provide an ideal setting to quantify transient bedrock incision. Primary evidence for transient incision on the Fortymile River comprises a single gravel-capped strath terrace that continuously flanks the lower ~170 km of the trunk river's ~285 km length, with incision depth increasing downstream (Yeend, 1996; Figure 1A-D). Tectonic quiescence of the Fortymile River region (Ruppert et al., 2008) suggests uniform and negligible rates of recent rock uplift throughout the drainage. Paleozoic to Mesozoic metamorphic, granitic, and volcanic bedrock units floor the Fortymile Basin, forming a landscape where expected rock strength, and hence erosivity, varies minimally (Foster, 1976). Historical mean annual precipitation in the Fortymile River basin is low, nearly uniform across the basin (Gibson, 2009), and likely represents typical conditions since Late Pliocene time (Ager et al., 1994). Finally, the Fortymile River drainage remained ice-free below ~1200 m elevation through several regional Quaternary glaciations (Weber and Wilson, 2012) with ~95% of the river network unmodified by glacial processes.

Evidence for Late Pliocene-Early Pleistocene Yukon River headwater capture provides an implicit but previously untested mechanism for abrupt Fortymile River base level lowering and consequent bedrock incision. Southeast-graded Miocene-Pliocene strath terraces flank the northwest-flowing modern Yukon River and define a paleo-drainage divide between Dawson City, Yukon and the Fortymile River outlet in Alaska (Duk-Rodkin et al., 2001; Jackson et al., 2009; Figure 1A-B). Regionally, outwash gravel deposits containing exotic, intracontinental-derived clasts mark the farthest extent of the Late Pliocene Cordilleran Ice Sheet (CIS) and abut geomorphic evidence of the coeval glacial Lake Yukon, which formed in response to ice sheet damming of the ancestral, south-flowing Yukon River. Duk-Rodkin et al. (2001) suggest that glacial Lake Yukon spilled west over the paleo-divide, captured the ice-dammed ancestral Yukon River headwaters and entrenched the modern course of the Yukon River (Figs. 1A, 2). At a site near the capture point (Figs. 1A, 2), Hidy et al. (2018) report a cosmogenic nuclide simple burial age of 2.84 $^{+0.22}/_{-0.19}$ Ma for the exotic-over-local gravel contact, and a cosmogenic exposure (and hence minimum) age of 1.12 $^{+0.44}/_{-0.36}$ Ma for a soil developed regionally at the top of CIS terrace stratigraphy. The cosmogenic ages bracket the timing of maximum CIS expansion and subsequent Yukon River capture, and agree with magnetostratigraphic and tephra data (Froese et al., 2000).

In this paper, we test whether Yukon River capture triggered bedrock incision in the Fortymile River, quantify the subsequent pace of landscape response across 10^4-10^6 y timescales, and demonstrate the efficacy of a simple stream power incision model.

COSMOGENIC METHODS

We use the cosmogenic ^{26}Al-^{10}Be isochron method (Balco and Rovey, 2008) to date the burial of the Fortymile River terrace gravel. The isochron method exploits the known in situ production ratio of ^{26}Al:^{10}Be atoms in quartz at Earth's surface, and the different rates at which the accumulated isotopes decay following deposition in a single stratigraphic horizon at depth sufficient to minimize post-burial nuclide production (i.e., >2 m; Balco and Rovey, 2008).

We collected samples (n = 6) from 3.2 to 3.5 m depth in a massive, ~25 m-thick fluvial gravel deposit underlying the high terrace tread at a site, informally called Clinton Creek, located ~7 km upstream of the Fortymile-Yukon River confluence (Fig. 1A). We sampled near the top of the terrace gravel to establish the timing of terrace abandonment.

We also quantify basin-scale erosion rates using ^{10}Be concentrations measured in quartz from modern river sand at six tributary outlets along the Fortymile River (Fig. 1A). We calculate the ^{10}Be production rate-weighted average elevation and latitude for each sample catchment, and evaluate ^{10}Be concentrations for erosion rates using the CRONUS Earth online calculator (Balco et al., 2008). Tributary erosion rate units (mm/ka) are numerically equivalent to incision rate units (m/Ma), but reflect the shorter timescale of integration. We prepared samples at the University of Vermont (Corbett et al., 2016) and measured $^{26}Al/^{27}Al$ and $^{10}Be/^{9}Be$ ratios at the Purdue Rare Isotope Measurement (PRIME) Laboratory (see Data Repository).

STREAM POWER METHODS

We extract Fortymile River trunk channel elevation, dimensionless channel slope (S), and drainage area (A, m^2) values from the 50 m/pixel National Elevation Database Alaska DEM, and compute indices of channel concavity (θ), reference concavity (θ_{ref}), and normalized channel steepness (k_{sn})(Wobus et al., 2006). We use a form of the slope-area relationship observed among equilibrium channels ($S = k_{sn}A^{-\theta_{ref}}$; Wobus et al., 2006) to project the headwater gradient downstream over a long-profile of terrace tread pixel elevations extracted from the Alaska DEM (terrace mapping updated from Weber and Wilson, 2012; Fig. 1A). We divide strath height by the terrace gravel age (~2.44 Ma) to infer minimum bedrock incision rates in the knickzone.

We calibrate and test the common stream power incision model (e.g., Whipple and Tucker, 1999) that approximates bedrock incision rate (I, m/y) as a function of A and S:

$$I = KA^mS^n \quad (1)$$

Positive constants m and n are derived from empirical I, θ_{ref}, and k_{sn} values. We discern two constant values for the dimensional coefficient of erosion K (units of m^{1-2m}; e.g., Whipple and Tucker, 1999) for scenarios of bedrock incision proportional to stream power and bed shear stress using a finite difference approach described in the Data Repository.

RESULTS

Clinton Creek cosmogenic ^{26}Al and ^{10}Be concentrations yield an isochron burial age of 2.44 ± 0.24 Ma (1σ, as with all uncertainties quoted in this paper) for the terrace gravel (Fig. 2). This age falls well within the age range of terrace gravels directly linked to the maximum CIS advance in the ancestral Yukon River headwater (1.12–2.84 Ma; Hidy et al., 2018). These equivalent ages permit correlation of the gravels across the ancestral Yukon River drainage divide (Figs. 1A, 2) and indicate an interval of regional aggradation under CIS climate-imposed sediment flux and discharge conditions (e.g., Hancock and Anderson, 2002). Ages of the Fortymile River terrace gravel and CIS-related gravels also constrain the onset timing of Fortymile River strath terrace abandonment and Yukon River headwater capture via glacial lake spillover, respectively. The correlative ages and the position of the Fortymile River outlet west of the capture point (Figs. 1A, 2), collectively imply that Fortymile River terrace abandonment at 2.44 ± 0.24 Ma and subsequent bedrock incision resulted from sustained base level lowering driven by Yukon River headwater capture during the maximum CIS advance after 2.84 Ma (Hidy et al., 2018).

Bedrock incision sets up to ~80% of the Fortymile basin relief structure (Fig. 3A) based on a 40-km-wide swath topographic profile centered on the studied river reaches

(Fig. 1A). Slope-area regressions quantify the high concavity and low gradient of the headwater reach ($\theta_{headwaters}$ = 0.62 ± 0.04; k_{sn} = 228), as well as the steeper linear downstream reach that we refer to as the knickzone ($\theta_{knickzone}$ = 0.009 ± 0.19; k_{sn} = 1120). Bin-averaged terrace tread elevations fall entirely within the 1σ range of the projected equilibrium headwater gradient (Fig. 3B), strongly suggesting a continuous pre-incision channel profile graded to an ancestral base level under CIS climate conditions, and representative of the relict landscape.

The depositional age and strath height at the Clinton Creek site imply time-averaged bedrock incision at a rate of 103 ± 25 m/Ma near the Fortymile-Yukon River confluence (Fig. 3C). Incision depth decreases to ~50 m near the upstream extent of the terrace (Fig. 3B), with inferred rates of bedrock incision decreasing upstream to 19 ± 4 m/Ma (Fig. 3C). ^{10}Be concentrations indicate that tributaries draining to the headwater reach (n = 2) eroded slowly and uniformly (9 ± 1 mm/ka) over the past 60–70 ka. In contrast, tributary erosion rates within the knickzone (n = 5) range from 18–14 ± 2 mm/ka (Fig. 3E), and reflect erosion over the past 20–30 ka.

For a stream power model in the form of (1) where n = 2/3 (incision linear in shear stress) or n = 1 (incision linear in stream power), uniform K values of 1.113 ± 0.004 $m^{0.2} \times 10^{-6}$ and 1.08 ± 0.02 $m^{-0.2} \times 10^{-6}$ best reproduce the observed knickzone profile, respectively (Fig. 4). Reported values of K fall within the published range of empirically determined values for granitic and metamorphic rocks (10^{-6} to 10^{-7} $m^{0.2}$/y; Stock and Montgomery, 1999). Linear regressions of the modeled and observed knickzone profile elevations show a correlative and nearly 1:1 relationship (Fig. 4).

DISCUSSION

DOI:10.1130/G40203.1

Bedrock incision resulting from Yukon River capture profoundly impacts the Fortymile River landscape. About 300 m of relief occurs in the gentle, concave, minimally incised headwater reach that has yet to “feel” the transient incision occurring in the knickzone. In contrast, basin relief nearly doubles downstream as a result of up to ~260 m of bedrock incision into the relict landscape of the strath terrace (Fig. 3A-B). Inferred bedrock incision rates decrease upstream along the knickzone (Fig. 3D), generally matching patterns of drainage area proportionality predicted by simple stream power models (Whipple and Tucker, 1999) and similar to other fluvial systems undergoing transient adjustment to base level lowering (Harkins et al., 2007).

Downstream variations in basin-scale erosion rate provide a signature of the stability or capture-related transience of the Fortymile River trunk channel elevation. Low basin-scale erosion rates observed in the relict landscape of the headwater reach reflect the background pace of tributary erosion, un-perturbed by transient knickzone incision. Accordingly, tributary erosion rates increase abruptly from the headwater into the knickzone by a factor of two (Fig. 3E). This increase suggests that the Fortymile River landscape is still responding, at a pace up to twice the background rate, to bedrock incision initiated at ~2.44 Ma. Within the knickzone, tributary erosion rates (14-18 +/- 2 mm/ka) intersect the lowest inferred rates of incision (17–19 ± 4 m/Ma) near the upstream extent of the knickzone, revealing a local match in the tempo of 10^4 y erosion set by 10^6 y incision (Fig. 3D-E). The erosion-incision rate intersection suggests recent tributary perturbation by the transient knickzone channel level, consistent with ongoing landscape adjustment.

Close agreement between observed and modeled knickzone profiles (Fig. 4) helps elucidate long-term Fortymile River incision processes. Consistent with the inferred downstream increase in incision rate (Fig. 3D) and headwater-to-knickzone increase in steepness (Fig. 3B-C), model results indicate that incision of the Fortymile River knickzone is largely a function of drainage area and channel slope. This apparent slope-area dependence implies that discharge stochasticity and dynamic channel width had little impact on bedrock incision averaged over 10^4-10^6 y. Moreover, we compute a uniform erosivity value (K) that appears to absorb the effect of spatial-temporal variations in rock strength, sediment flux, and erosion mechanics. Correlation between observed and modeled profiles (Fig. 4) indicates that under boundary conditions exemplified by the Fortymile River, simple stream power models can approximate patterns of transient bedrock incision at 10^4-10^6 y timescales.

CONCLUSIONS

Yukon River headwater capture, forced by the Plio-Pleistocene CIS maximum, triggered Fortymile River terrace abandonment via base level lowering at 2.44 ± 0.24 Ma. Subsequent fluvial downcutting profoundly altered the architecture of the Fortymile River basin, where bedrock incision within a broad knickzone nearly doubles the relief of the relict landscape. The Fortymile River landscape continues to respond to the drainage capture, as evidenced by elevated 10^4 y basin-scale erosion rates that intersect 10^6 y inferred bedrock incision rates near the upstream extent of the knickzone. The pristine geomorphic record of pre-incision conditions allows us to tune a simple stream power incision model that, unimpeded by climatic, tectonic, or lithologic complexity, closely reproduces the observed knickzone channel profile. We thus propose that, under these consistent boundary conditions, transient bedrock incision over 10^4-10^6 y timescales may be well-approximated as a simple power law function of drainage area and slope.

ACKNOWLEDGMENTS

We thank S. Gallen, G. Hancock, A. Hidy, S. Johnstone, T. Pico and R. Witter for thoughtful discussions; E. Shea for rock lab access; C. Bacon, J. Bond, A. Cyr, B. Goehring, J. Perkins and an anonymous referee for constructive reviews of this manuscript; and the USGS Mineral Resources Program for funding. Any use of trade, firm, or product names is for descriptive purposes only and does not imply endorsement by the U.S. Government.

REFERENCES CITED

Ager, T.A., Matthews, J.V., Jr., and Yeend, W., 1994, Pliocene terrace gravels of the ancestral Yukon River near Circle, Alaska: Palynology, paleobotany, paleoenvironmental reconstruction and regional correlation: Quaternary International, v. 22–23, p. 185–206, https://doi.org/10.1016/1040-6182(94)90012-4.

Balco, G., Stone, J.O., Lifton, N.A., and Dunai, T.J., 2008, A complete and easily accessible means of calculating surface exposure ages or erosion rates from ^{10}Be and ^{26}Al measurements: Quaternary Geochronology, v. 3, p. 174–195, https://doi.org/10.1016/j.quageo.2007.12.001.

Balco, G., and Rovey, C.W., 2008, An isochron method for cosmogenic-nuclide dating of buried soils and sediments: American Journal of Science, v. 308, p. 1083–1114, https://doi.org/10.2475/10.2008.02.

Corbett, L.B., Bierman, P.R., and Rood, D.H., 2016, An approach for optimizing in situ cosmogenic 10 Be sample preparation: Quaternary Geochronology, v. 33, p. 24–34, https://doi.org/10.1016/j.quageo.2016.02.001.

DiBiase, R.A., and Whipple, K.X., 2011, The influence of erosion thresholds and runoff variability on the relationships among topography, climate, and erosion rate: Journal of Geophysical Research, Earth Surface, v. 116, p. F4, 10.1029/2011JF002095.

Duk-Rodkin, A., Barendregt, R.W., White, J.M., and Singhroy, V.H., 2001, Geologic evolution of the Yukon River: implications for placer gold: Quaternary International, v. 82, p. 5–31, https://doi.org/10.1016/S1040-6182(01)00006-4.

Duvall, A., Kirby, E., and Burbank, D., 2004, Tectonic and lithologic controls on bedrock channel profiles and processes in coastal California: Journal of Geophysical Research, Earth Surface, v. 109, p. F3, 10.1029/2003JF000086.

Froese, D.G., Barendregt, R.W., Enkin, R.J., and Baker, J., 2000, Paleomagnetic evidence for multiple late Pliocene-early Pleistocene glaciations in the Klondike area, Yukon Territory: Canadian Journal of Earth Sciences, v. 37, p. 863–877, https://doi.org/10.1139/e00-014.

Foster, H.L., 1976, Geologic map of the Eagle quadrangle, Alaska: U.S. Geological Survey Miscellaneous Investigations Series Map 1–922, scale 1:250,000.

Gibson, W., 2009, Mean Precipitation for Alaska 1971–2000: National Park Service, https://irma.nps.gov/DataStore/Reference/Profile/2170508 (accessed December 2017).

Harkins, N., Kirby, E., Heimsath, A., Robinson, R., and Reiser, U., 2007, Transient fluvial incision in the headwaters of the Yellow River, northeastern Tibet, China: Journal of Geophysical Research, Earth Surface, v. 112, p. F03S04, 10.1029/2006JF000570.

Hancock, G.S., and Anderson, R.S., 2002, Numerical modeling of fluvial strath-terrace formation in response to oscillating climate: Geological Society of America Bulletin, v. 114, p. 1131–1142.

Hidy, A.J., Gosse, J.C., Sanborn, P., and Froese, D.G., 2018, Age-erosion constraints on an Early Pleistocene paleosol in Yukon, Canada, with profiles of ^{10}Be and ^{26}Al: Evidence for a significant loess cover effect on cosmogenic nuclide production rates: Catena, v. 165, p. 260–271, https://doi.org/10.1016/j.catena.2018.02.009.

Jackson, L.E., Jr., Froese, D.G., Huscroft, C.A., Nelson, F.E., Westgate, J.A., Telka, A.M ., Shimamura, K., and Rotheisler, P.N., 2009, Surficial geology and late Cenozoic history of the Stewart River and northern Stevenson Ridge map areas, west-central Yukon Territory: Geological Survey of Canada, Open File, 6059, 414 p. doi:https://doi.org/10.4095/248232.

Kirby, E., and Whipple, K., 2001, Quantifying differential rock-uplift rates via stream profile analysis: Geology, v. 29, p. 415–418, https://doi.org/10.1130/0091-7613(2001)029<0415:QDRURV>2.0.CO;2.

Lague, D., 2014, The stream power river incision model: evidence, theory and beyond: Earth Surface Processes and Landforms, v. 39, p. 38–61, https://doi.org/10.1002/esp.3462.

Ruppert, N.A., Ridgway, K.D., Freymueller, J.T., Cross, R.S., and Hansen, R.A., 2008, Active tectonics of interior Alaska: Seismicity, GPS geodesy, and local geomorphology: Active Tectonics and Seismic Potential of Alaska, p. 109–133, doi:10.1029/179GM06.

Scherler, D., DiBiase, R.A., Fisher, G.B., and Avouac, J.P., 2017, Testing monsoonal controls on bedrock river incision in the Himalaya and Eastern Tibet with a stochastic-threshold stream power model: Journal of Geophysical Research, Earth Surface, v. 122, p. 1389–1429, https://doi.org/10.1002/2016JF004011.

Sklar, L., and Dietrich, W.E., 1998, River longitudinal profiles and bedrock incision models: Stream power and the influence of sediment supply, *in* Tinkler, K.J., and Wohl, E.E., eds., Rivers Over Rock: Fluvial Processes in Bedrock Channels: American Geophysical Union, v. 1, p. 237–260, doi:https://doi.org/10.1029/GM107p0237.

Stock, J.D., and Montgomery, D.R., 1999, Geologic constraints on bedrock river incision using the stream power law: Journal of Geophysical Research, Solid Earth, v. 104, p. 4983–4993, https://doi.org/10.1029/98JB02139.

Weber, F.R., and Wilson, F.H., 2012, Map showing extent of glaciation in the Eagle quadrangle, east-central Alaska: U.S. Geological Survey Open-File Report 2012–1138, scale 1:250,000.

Whipple, K.X., and Tucker, G.E., 1999, Dynamics of the stream-power river incision model: Implications for height limits of mountain ranges, landscape response timescales, and research needs: Journal of Geophysical Research, Solid Earth, v. 104, p. 17661–17674, https://doi.org/10.1029/1999JB900120.

Whipple, K.X., DiBiase, R.A., and Crosby, B.T., 2013, Bedrock rivers, *in* Shroder, J., and Wohl, E., eds., Treatise on Geomorphology: Fluvial Geomorphology: San

Diego, California, Academic Press, v. 9, p. 550–573, https://doi.org/10.1016/B978-0-12-374739-6.00254-2.

Wobus, C., Whipple, K.X., Kirby, E., Snyder, N., Johnson, J., Spyropolou, K., Crosby, B., Sheehan, D., and Willett, S.D., 2006, Tectonics from topography: Procedures, promise, and pitfalls: Geological Society of America Special Paper, v. 398, p. 55, 10.1130/2006.2398(04).

Yeend, W.E., 1996, Gold placers of the historical Fortymile River region, Alaska: U.S. Geological Survey Bulletin 2125, 75 p.

FIGURE CAPTIONS

Figure 1. Study area. (A) Fortymile River basin, with investigated West Fork and main stem trunk channels. Inset depicts modern Yukon River basin. DC - Dawson City, Yukon. (B) schematic profile A-A' (on Fig. 1A) depicting simplified record of Mio-Pliocene Yukon River capture, modified from Duk-Rodkin et al. (2001). (C) minimally incised West Fork headwaters. (D) deeply incised main stem, B and C locations on Figure 1A.

Figure 2. Cosmogenic isochron burial age plot for samples collected at the Clinton Creek high terrace gravel site.

Figure 3. Long profile projections of Fortymile River data. (A) Max and min elevations in a 40 km-wide swath (Fig. 1A), with profiles of tributaries sampled for erosion rates. Swath distance scaled to river distance by ~1.2x. (B) Long profiles of the studied trunk

channels, high strath terrace tread, and projected headwater. Smoothed channel profile in blue, raw profile in gray, steps in profile occur at major tributary junctions. 1σ headwater profile projection uncertainty in black dashed lines. (C) Log slope-log area regressions used to derive steepness and concavity for the headwater and knickzone reaches. Black squares are log-bin averaged data, gray crosses are data smoothed on 10 km window, black and gray lines depict the regressed and reference concavities, respectively (Wobus et al., 2006). (D) Inferred rates of knickzone bedrock incision. Light gray dots are raw, dark gray dots are 10 km bin averaged with 1σ uncertainty, yellow dot is point rate calculated for the Clinton Creek site. (E) ^{10}Be-based rates of tributary erosion. Note that the vertical scales of (D) and (E) overlap permissibly given unit equivalence.

Figure 4. Regressions of modeled against observed knickzone channel elevations on 10 km distance bins. Inset shows modeled elevations over the smoothed DEM long profile.

1GSA Data Repository item 2018xxx, xxxxxxxx, is available online at http://www.geosociety.org/datarepository/2018/ or on request from editing@geosociety.org.

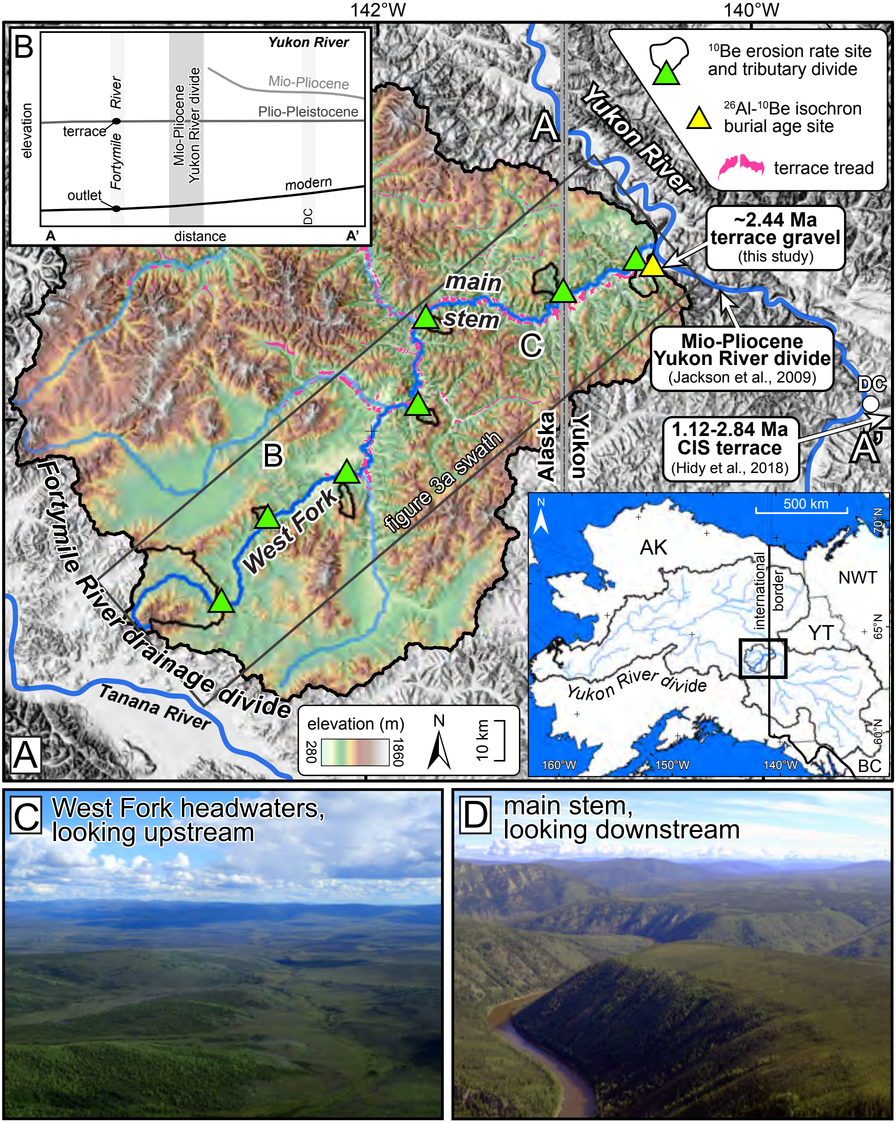
142°W
140°W
64°N
B
Yukon River
Mio-Pliocene
Plio-Pleistocene
modern
elevation
terrace
outlet
Fortymile River
Mio-Pliocene Yukon River divide
DC
A
distance
A'
10Be erosion rate site and tributary divide
26Al-10Be isochron burial age site
terrace tread
Yukon River
A
~2.44 Ma terrace gravel
(this study)
Mio-Pliocene Yukon River divide
(Jackson et al., 2009)
1.12-2.84 Ma CIS terrace
(Hidy et al., 2018)
DC
A'
main
stem
C
B
West Fork
figure 3a swath
Alaska
Yukon
Fortymile River drainage divide
Tanana River
elevation (m)
280
1860
N
10 km
A
N
500 km
AK
NWT
YT
international border
Yukon River divide
70°N
65°N
60°N
160°W
150°W
140°W
BC
C
West Fork headwaters, looking upstream
D
main stem, looking downstream

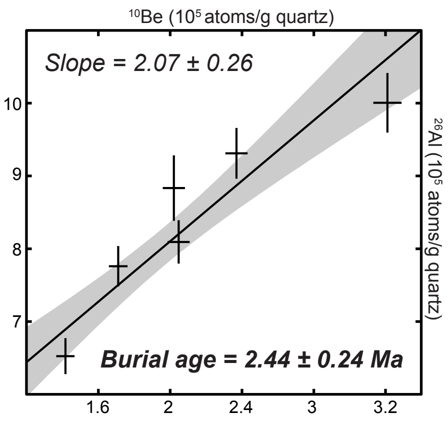

¹⁰Be (10⁵ atoms/g quartz)
Slope = 2.07 ± 0.26
Burial age = 2.44 ± 0.24 Ma
²⁶Al (10⁵ atoms/g quartz)
10
9
8
7
1.6
2
2.4
3
3.2

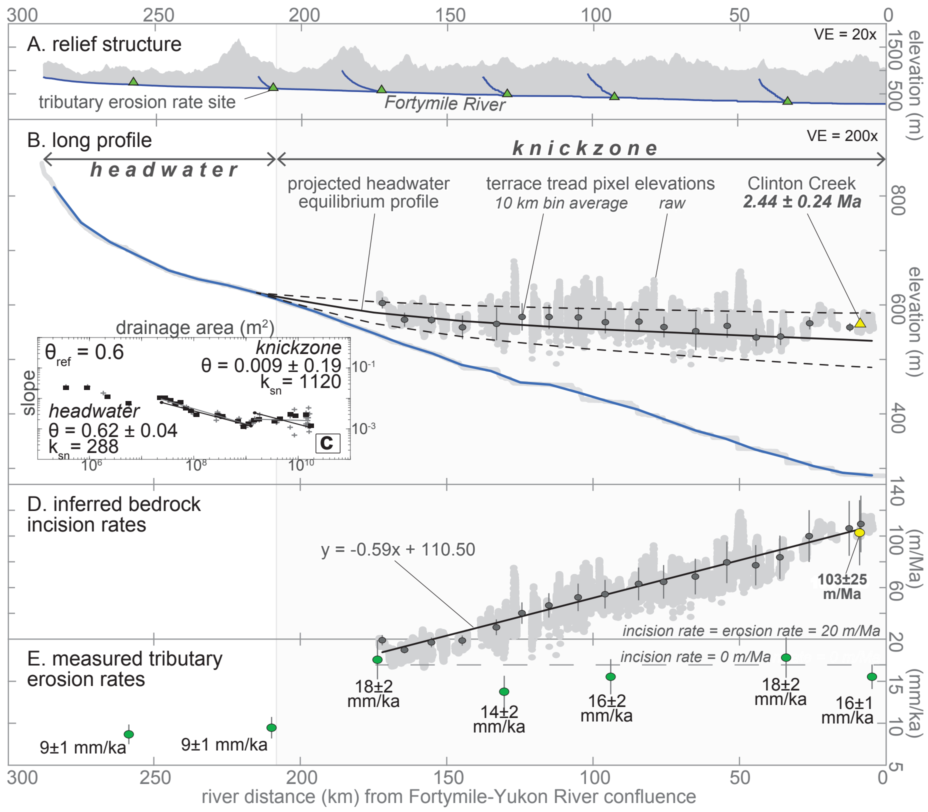

A. relief structure
VE = 20x
tributary erosion rate site
Fortymile River
elevation (m)
B. long profile
VE = 200x
headwater
knickzone
projected headwater equilibrium profile
terrace tread pixel elevations
10 km bin average
raw
Clinton Creek
2.44 ± 0.24 Ma
drainage area (m²)
θ_{ref} = 0.6
knickzone
θ = 0.009 ± 0.19
k_{sn} = 1120
slope
headwater
θ = 0.62 ± 0.04
k_{sn} = 288
C
D. inferred bedrock incision rates
y = -0.59x + 110.50
103±25 m/Ma
incision rate = erosion rate = 20 m/Ma
(m/Ma)
E. measured tributary erosion rates
incision rate = 0 m/Ma
18±2 mm/ka
14±2 mm/ka
16±2 mm/ka
18±2 mm/ka
16±1 mm/ka
9±1 mm/ka
9±1 mm/ka
(mm/ka)
river distance (km) from Fortymile-Yukon River confluence

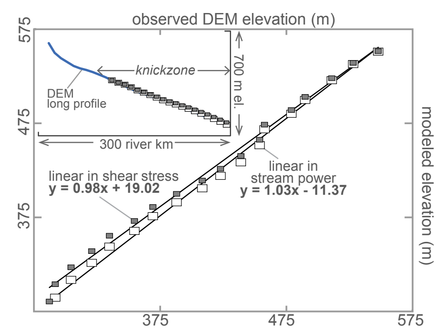
observed DEM elevation (m)
575
475
375
575
475
375
575
modeled elevation (m)
knickzone
700 m el.
DEM
long profile
300 river km
linear in shear stress
y = 0.98x + 19.02
linear in
stream power
y = 1.03x - 11.37

Data Repository

Ongoing transient bedrock incision of the Fortymile River driven by Late Pliocene Yukon River capture, eastern Alaska and Yukon, Canada

Adrian Bender[1], Richard Lease[1], Lee Corbett[2], Paul Bierman[2] and Marc W. Caffee[3]

[1]U.S. Geological Survey Alaska Science Center, Anchorage, Alaska, 99508; email: abender@usgs.gov

[2]University of Vermont, Department of Geology, Burlington, VT 05405

[3]Department of Physics and Astronomy, and Department of Earth, Atmospheric, and Planetary Sciences Purdue University, 525 Northwestern Avenue, West Lafayette, IN 47907

EXPANDED METHODS

Disclaimer

Any use of trade, firm, or product names is for descriptive purposes only and does not imply endorsement by the U.S. Government.

Cosmogenic isochron burial dating

The isochron method (Balco and Rovey, 2008) generally requires sampling quartz-bearing material spanning a range of pre-burial isotope concentrations from a single horizon (indicative of common burial history) buried by several m of sediment (sufficient to minimize post-burial production). We satisfy these sampling requirements at a shallow pit (sample horizon from 3.2-3.5 m depth) in the Fortymile River terrace gravel at a site we refer to as Clinton Creek located ~7 km upstream of the Fortymile-Yukon River confluence (Fig. DR1). The isochron method involves fitting a line to measured nuclide concentrations and analytical uncertainties, with ^{10}Be and ^{26}Al on the x- and y-axes, respectively (e.g., Bender et al., 2016). We use the York regression method housed in Isoplot 4.15 (http://www.bgc.org/isoplot_etc/isoplot.html) that considers x and y uncertainties (e.g., Mahon, 1996). The slope (R_{meas}) of the line fit to the measured concentrations reflects the deviation from the surface ^{26}Al: ^{10}Be production ratio (R_{init}; Fig. DR2). The slope deviation depends on isotope half-life and duration of post-burial decay, so the burial age (t_b) is calculated as:

$$t_b = -ln(R_{meas}/R_{init})/(\lambda_{26} - \lambda_{10}) \qquad (1)$$

In keeping with other published applications of the isochron method (c.f. Schaller et al., 2016) we use the commonly accepted but poorly empirically constrained R_{init} value of 6.75 (e.g., Corbett et al, 2017). Decay constants λ_{26} ($9.83 \pm 0.25 \times 10^{-7}$/yr) and λ_{10} ($5.00 \pm 0.26 \times 10^{-7}$/yr) equate with half-lives of 0.705 Myr for ^{26}Al (Nishiizumi, 2004) and 1.387 Myr for ^{10}Be (c.f., Chmeleff et al., 2010).

A key goal for the Fortymile River terrace gravel age is comparison and correlation with the Cordilleran Ice Sheet (CIS)-related gravel dated by Hidy and others (2013, 2018) between 1.12 $^{+0.44}/_{-0.36}$ and 2.84 $^{+0.22}/_{-0.19}$ Ma. Comparing these ages requires parallel comparison of the respective methods, and the processes being dated. We use the same laboratory standards and decay constants assumed in the ^{26}Al-^{10}Be ages of Hidy and others (2013, 2018), but our sampling and computational approaches differ. Whereas we use the isochron approach (Balco and Rovey, 2008), Hidy and others (2013, 2018) calculate (a) a 2.84 $^{+0.22}/_{-0.19}$ Ma simple depositional age based on burial plot analysis of clasts from different depths across the CIS-over-local gravel contact, and (b) a 1.12 $^{+0.44}/_{-0.36}$ Ma depth profile exposure age of soil developed at the terrace surface of the CIS gravel. These ages bracket the onset of CIS terrace gravel deposition (~2.84 Ma) and the stabilization of the terrace surface (~1.12 Ma) such that a depositional age of terrace gravel that falls within this range correlates temporally to aggradation-prone sediment flux and discharge conditions imposed by the CIS climate (e.g., Hancock and Anderson, 2002). Moreover, Hidy and others (2018) interpret lower-than-expected in-situ isotope ratios in their exposure age depth profile as the result of isotope production impeded by temporally intermittent loess cover. We note that because the isochron technique relies on the pre-burial isotope inheritance of each sample, and not in situ-produced concentrations analyzed by depth profile techniques, the depositional age we compute (via the isochron technique) is not sensitive to intermittent burial by loess or other deposits.

^{10}Be-based tributary erosion rates

We quantify basin-averaged erosion rates using ^{10}Be concentrations measured in quartz from modern river sand (250-850 μm) at six tributary outlets on the Fortymile River. ^{10}Be accumulates in quartz at Earth's surface to depths commensurate with cosmic ray e-folding length (~0.6 m in rock), at rates determined largely by latitude and altitude (e.g., Lal, 1991; Stone, 2000) and inversely proportional to erosion rate (e.g., Brown et al., 1995; Granger et al., 1996; Bierman and Steig, 1996). Dividing the ^{10}Be

production depth by a given measured erosion rate thus estimates the duration of erosion at the measured rate. Given similar rock type and durability throughout the Fortymile River basin and minimal lithologic variation within the sampled tributary catchments (Foster, 1976), we make the simple assumption that quartz sampled at the 250-850 µm grain size range is well-mixed and represents erosion throughout the tributary catchment upstream. We calculate the ^{10}Be production rate-weighted average elevation and latitude for each sample catchment (e.g., Brown et al., 1995; Granger et al., 1996; Bierman and Steig, 1996; Portenga and Bierman, 2011), and use the CRONUS online calculator (https://hess.ess.washington.edu/) to assess erosion rates based on ^{10}Be concentrations at each outlet (Balco et al., 2008). Topographic shielding minimally impacts ^{10}Be production rates because topography is relatively open in the basins we sample, with average hillslopes of 6° to 16° (e.g., Bierman and Steig, 1996). Similarly, the mean winter snow depth of <50 cm measured at Fortymile Basin SNOTEL sites 1275 and 1189 (https://wcc.sc.egov.usda.gov/nwcc/) confers shielding effects that contribute ~1-3% uncertainty by some estimates (Gosse and Phillips, 2001). Schildgen and others (2005) show that, in certain locations, snow cover can reduce the long-term (15.5 ka) ^{10}Be production rate up to 14%, and suggest that using contemporary climate data to estimate snow shielding may inject systematic error into ^{10}Be production assessment and derivative calculations. Instead of attempting to explicitly treat snow or topographic shielding effects, we subsume the expected minimal snow and topographic shielding effects on ^{10}Be production rate by directly adding 5% of each CRONUS-reported rate to the attendant reported uncertainty.

Bedrock incision

We infer bedrock incision rates by dividing strath height over the terrace gravel age (~2.44 Ma). We compute strath height as the difference between channel elevation, gravel thickness (tread to strath), and terrace tread (gravel top) elevation. We measured terrace gravel thickness (range 5 to 25 m) using a laser range finder or tape measure at four sites along the studied river reach, among which we observe linear upstream thinning ($y = -0.11x + 24$ where y represents gravel thickness in meters and x represents river distance in kilometers; $R^2 = 0.95$) that we use to extrapolate gravel thickness along the river. We use the active channel as a vertical datum for incision given that (a) the active channel occupies an elevation between the bedrock channel bed and flood stage levels at which lateral and vertical incision likely occur (e.g., Lague, 2014), (b) the ~2.44 Ma time interval over which we average bedrock incision approaches the upper limit of the time range over which bedrock incision rates may decrease as a function of age (Finnegan et al., 2014; Gallen et al., 2015), and (c) our channel profile analysis indicates that the entire knickzone remains in a transient state wherein active channel adjustment via bedrock incision likely continues to the present. Finally, we acknowledge that using a single terrace gravel age to infer rates of incision implicitly neglects the probable upstream decrease in gravel age that should reflect progressive terrace abandonment downstream of a headward-propagating knickzone, and therefore consider as minima the incision rates thusly inferred.

Stream power model

We analyze the Fortymile River longitudinal profile using the relationship between dimensionless channel slope (S) and drainage area (A, m^2) observed among equilibrium-state channels (e.g., Sklar and Dietrich, 1998):

$$S = k_s A^{-\theta} \qquad (2)$$

Indices of channel steepness (k_s) and concavity (θ) represent the y-intercept and slope of a logarithmic regression of A and S, respectively. Fixing θ at a reference value (θ_{ref}) allows assessment of a channel steepness index normalized to drainage area (k_{sn})(Wobus et al, 2006), permitting quantitative comparison of geometrically distinct river reaches:

$$S = k_{sn} A^{-\theta ref} \qquad (3)$$

We use knickzone incision rates to calibrate and test a common stream power incision model (e.g., Whipple and Tucker, 1999) that approximates bedrock incision rate (*I*, m/y) as a power law function of A and S:

$$I = KA^m S^n \qquad (4)$$

Positive constants *m* and *n* reflect channel morphology, and *K* represents a dimensional coefficient of erosion (units of m^{1-2m})(e.g., Whipple and Tucker, 1999). The solution for *S* implicit in (4) takes the form of (3), assuming constant downstream *K* and *n*, such that k_{sn} and θ_{ref} equal the stream power terms $(I/K)^{1/n}$ and *m/n*, respectively. We use the term compatibility between (3) and (4) to calculate *K*, *m*, and *n* based on headwaters k_{sn} value of 228 and $m/n = \theta_{ref} = 0.6 \sim \theta_{headwaters}$ (the high end of model-predicted m/n values, 0.35 to 0.6; Whipple and Tucker, 1999).

We infer *I* from terrace tread elevation, gravel thickness, active channel elevation and the terrace gravel age averaged on 10 km river distance bins along the Fortymile River knickzone, and use the bin-averaged incision rates to solve for *K* linearly proportional to basal shear stress ($n = 2/3$ and therefore $m = 2/5$) and stream power ($n = 1$ and therefore $m = 3/5$). To discern a suitable, constant value of *K*, we iteratively test values of *K* within the range published by Stock and Montgomery (1999) in an initial coarse search, and tighten the search interval for a fine search at the order of magnitude scale. We rearrange equation (4) to solve for knickzone channel elevation by treating *S* as the downstream change in elevation over distance, and systematically model the knickzone reach of the Fortymile River long profile for *K* values within the apparent order of magnitude that the suitable value of *K* resides. We converge on a suitable *K* value by minimizing the difference between regression equations from linear fits of the 10 km distance-binned modeled channel elevations against distance (for cases where bedrock incision is linearly proportional to shear stress and stream power) and the linear elevation-distance relationship computed for the knickzone ($y = 1.621x + 267.5$). We calculate absolute differences in regression statistics and collect and plot each against the corresponding value of *K*, fitting lines that slope positively and negatively toward x-intercepts that bracket the best value of *K.* We use the linear fits (Fig. DR3) to calculate four values of *K* for both the stream power and shear stress cases, and average the values (which generally vary at the second or third decimal place) to ascertain a single uniform *K* value for each case.

TABLES

FIGURES

Table DR1: ^{10}Be data

Analysis	Site	latitude	longitude*	DEM elevation (m)**	sample	sub-sample	sample type***	material type	Quartz Mass (g)	Mass of ^{9}Be Added (μg)****	AMS Cathode Number	Measured ^{10}Be/^{9}Be Ratio*****	Measured ^{10}Be/^{9}Be Ratio uncertainty*****	Background-Corrected ^{10}Be/^{9}Be Ratio	Background-Corrected ^{10}Be/^{9}Be Ratio Uncertainty	^{10}Be Concentration (atoms/g)	^{10}Be Concentration Uncertainty (atoms/g)
isochron burial age	Clinton Creek	64.37448	-140.59348	566	16ALR247	1	c	quartz	21.0	241.0	144600	2.65E-13	8.10E-15	2.64E-13	8.12E-15	2.02E+05	6.22E+03
						2	c	quartz	20.9	240.3	144602	1.85E-13	6.65E-15	1.84E-13	6.67E-15	1.42E+05	5.13E+03
						7	c	quartz	20.5	240.8	144603	4.10E-13	1.00E-14	4.09E-13	1.00E-14	3.21E+05	7.87E+03
						9	c	quartz	21.7	241.5	144604	2.76E-13	8.25E-15	2.75E-13	8.27E-15	2.05E+05	6.15E+03
						16A	p	mix	21.8	241.3	144605	2.32E-13	6.99E-15	2.31E-13	7.02E-15	1.71E+05	5.20E+03
						16B	s	mix	21.4	241.7	144606	3.16E-13	8.21E-15	3.15E-13	8.23E-15	2.37E+05	6.20E+03
erosion rate	Sam Patch	64.31638	-141.00849	331	16ALR216	--	rs	mix	18.0	242.0	142742	3.61E-13	1.01E-14	3.60E-13	1.01E-14	3.24E+05	9.11E+03
	Jet Boat	64.25529	-141.72489	438	16ALR220	--	rs	mix	11.6	241.1	142743	2.81E-13	7.26E-15	2.80E-13	7.28E-15	3.88E+05	1.01E+04
	Big Burn	63.90196	-142.12326	548	16ALR225	--	rs	mix	20.0	241.0	142744	4.33E-13	9.04E-15	4.32E-13	9.06E-15	3.47E+05	7.28E+03
	Bear Paw	63.79564	-142.52548	622	16ALR227	--	rs	mix	13.8	240.9	142746	5.26E-13	1.05E-14	5.25E-13	1.06E-14	6.15E+05	1.24E+04
	Tussock	63.60166	-142.75092	670	16ALR228	--	rs	mix	19.7	241.5	142747	7.40E-13	1.37E-14	7.39E-13	1.37E-14	6.04E+05	1.12E+04
	Maiden Ck	64.38262	-140.62373	315	16ALR246	--	rs	mix	15.5	241.1	142748	2.81E-13	7.62E-15	2.80E-13	7.64E-15	2.92E+05	7.95E+03
	Wall Street Ck	64.05824	-141.76432	481	16ALR248	--	rs	mix	11.2	240.8	142749	3.01E-13	1.02E-14	3.00E-13	1.02E-14	4.32E+05	1.47E+04

^{10}Be samples were processed in three batches containing two blanks each. Blanks (n=6) have an average ^{10}Be/^{9}Be ratio of 8.49E-16 ± 5.45E-16 (Table DR5). Uncertainty in blanks was added quadratically. Quoted uncertainties represent the 1σ range.

*Projection: NAD_1983_Alaska_Albers

**Elevation from the National Elevation Database Alaska DEM, available by searching https://viewer.nationalmap.gov/basic/

***c = clast, p = amalgamated matrix pebbles, s = amalgamated matrix sand, rs = amalgamated modern river sand

****^{9}Be was added through a beryl carrier made at University of Vermont.

*****Isotopic analysis was conducted at PRIME Laboratory; ratios were normalized against standard 07KNSTD3110 with an assumed ratio of 2850 x 10^{-15} (Nishiizumi et al., 2007).

Table DR2: ^{26}Al data

Analysis	Site	latitude*	longitude*	DEM elevation (m)**	sample	sub-sample	sample type***	material type	Quartz Mass (g)	Total ^{27}Al Quantified by ICP-OES (μg)****	AMS Cathode Number	Measured ^{26}Al/^{27}Al Ratio*****	Measured ^{26}Al/^{27}Al Ratio Uncertainty*****	Background-Corrected ^{26}Al/^{27}Al Ratio	Background-Corrected ^{26}Al/^{27}Al Ratio Uncertainty	^{26}Al Concentration (atoms/g)	^{26}Al Concentration Uncertainty (atoms/g)
isochron burial age	Clinton Creek	64.37448	-140.59348	566	16ALR247	1	c	quartz	21.0	1446	144630	5.76E-13	2.93E-14	5.75E-13	2.93E-14	8.83E+05	4.49E+04
						2	c	quartz	20.9	1481	144632	4.13E-13	1.56E-14	4.12E-13	1.56E-14	6.52E+05	2.47E+04
						7	c	quartz	20.5	1749	144633	5.26E-13	2.15E-14	5.25E-13	2.15E-14	1.00E+06	4.10E+04
						9	c	quartz	21.7	1486	144634	5.30E-13	1.94E-14	5.30E-13	1.94E-14	8.09E+05	2.97E+04
						16A	p	mix	21.8	1571	144635	4.82E-13	1.72E-14	4.81E-13	1.72E-14	7.76E+05	2.77E+04
						16B	s	mix	21.4	2604	144636	3.44E-13	1.28E-14	3.43E-13	1.28E-14	9.31E+05	3.48E+04

^{26}Al samples were processed in two batches along with a total of five blanks. Blanks (n=5) have an average ^{26}Al/^{27}Al ratio of 7.67E-16 ± 4.68E-16 (Table DR5). Uncertainty in blanks was added quadratically. Quoted uncertainties represent the 1σ range.

*Projection: NAD_1983_Alaska_Albers

**Elevation from the National Elevation Database Alaska DEM, available by searching https://viewer.nationalmap.gov/basic/

***c = clast, p = amalgamated matrix pebbles, s = amalgamated matrix sand

****^{27}Al was added only to samples with insufficient total Al through commercial SPEX ICP standard with a concentration of 1000 μg mL-1. The total here reflects the sum of Al added through carrier and native Al in quartz.

*****Isotopic analysis was conducted at PRIME Laboratory; ratios were normalized against standard KNSTD with an assumed ratio of 1.818 x 10^{-12} (Nishiizumi et al., 2004).

Table DR3: Basin-average erosion rate data submitted to CRONUS

Sample name	*Latitude	*Longitude	*Elevation (m)	Elevation flag	Sample thickness (cm)	Sample density (g/cm3)	Shielding correction	^{10}Be concentration (atoms/g)	Uncertainty in ^{10}Be concentration (atoms/g)**	Name of Be-10 standardization	^{26}Al concentration (atoms/g)	Uncertainty in ^{26}Al concentration (atoms/g)	Name of Al-26 standardization
ALR216	64.37094	-141.05040	769	std	1	2.7	1	3.24E+05	9.11E+03	07KNSTD	0	0	KNSTD
ALR220	64.22979	-141.63644	831	std	1	2.7	1	3.88E+05	1.01E+04	07KNSTD	0	0	KNSTD
ALR225	63.84553	-142.10678	838	std	1	2.7	1	3.47E+05	7.28E+03	07KNSTD	0	0	KNSTD
ALR227	63.81671	-142.54467	818	std	1	2.7	1	6.15E+05	1.24E+04	07KNSTD	0	0	KNSTD
ALR228	63.62325	-142.81789	700	std	1	2.7	1	6.04E+05	1.12E+04	07KNSTD	0	0	KNSTD
ALR246	64.37084	-140.58320	543	std	1	2.7	1	2.92E+05	7.95E+03	07KNSTD	0	0	KNSTD
ALR248	64.04259	-141.70429	819	std	1	2.7	1	4.32E+05	1.47E+04	07KNSTD	0	0	KNSTD

*production rate weighted (e.g., Portenga and Bierman, 2011)

ainties represent the 1σ range.

Table DR4: Basin-average erosion rate results from CRONUS*

Sample name	Shielding factor	Production rate (muons) (atoms/g/yr)	internal uncertainty (m/Myr)	Erosion rate ((g/cm^2)/yr)	Erosion rate (m/Myr)	External uncertainty (m/Myr)	Production rate (spallation) ((atoms/g)/yr)
ALR216	1	0.10	0.52	4.81E-03	17.82	1.51	8.97
ALR220	1	0.10	0.42	4.20E-03	15.54	1.32	9.49
ALR225	1	0.10	0.38	4.74E-03	17.57	1.46	9.55
ALR227	1	0.10	0.20	2.56E-03	9.47	0.81	9.37
ALR228	1	0.10	0.17	2.34E-03	8.68	0.74	8.42
ALR246	1	0.09	0.46	4.38E-03	16.23	1.36	7.26
ALR248	1	0.10	0.49	3.71E-03	13.76	1.21	9.38

*Calculated May 6, 2018 at https://hess.ess.washington.edu using wrapper script v2.3, main calculator v2.1, objective function v2.0, constants v2.3, muons v1.1 and the Lal(1991)/Stone(2000) global production rate scaling scheme for spallation.

Table DR5: ^{10}Be and ^{26}Al blank ratios*

^{10}Be					***^{26}Al***				
Blank Name	UVM Batch Number	PRIME Cathode Number	^{10}Be/^{9}Be Ratio	^{10}Be/^{9}Be Ratio Uncertainty	Blank Name	UVM Batch Number	PRIME Cathode Number	^{26}Al/^{27}Al Ratio	^{26}Al/^{27}Al Ratio Uncertainty
BLK	607	142745	1.16E-15	4.11E-16	BLK	607	144629	1.19E-15	9.33E-16
BLKX	607	144601	1.24E-15	6.11E-16	BLKX	607	144631	BDL**	3.41E-16
BLK	608	144608	2.33E-16	3.36E-16	BLK	608	144638	6.99E-16	6.70E-16
BLKX	608	144614	4.85E-16	4.65E-16	BLKX	608	144644	1.08E-15	1.05E-15
BLK	609	144621	1.57E-15	4.98E-16	BLK	613	097387	8.69E-16	8.32E-16
BLKX	609	144627	4.02E-16	3.16E-16	--	--	--	--	--

*Samples generally processed with two blanks per batch. Blank corrections use an average of the blank ratios rather than batch-by-batch correction.

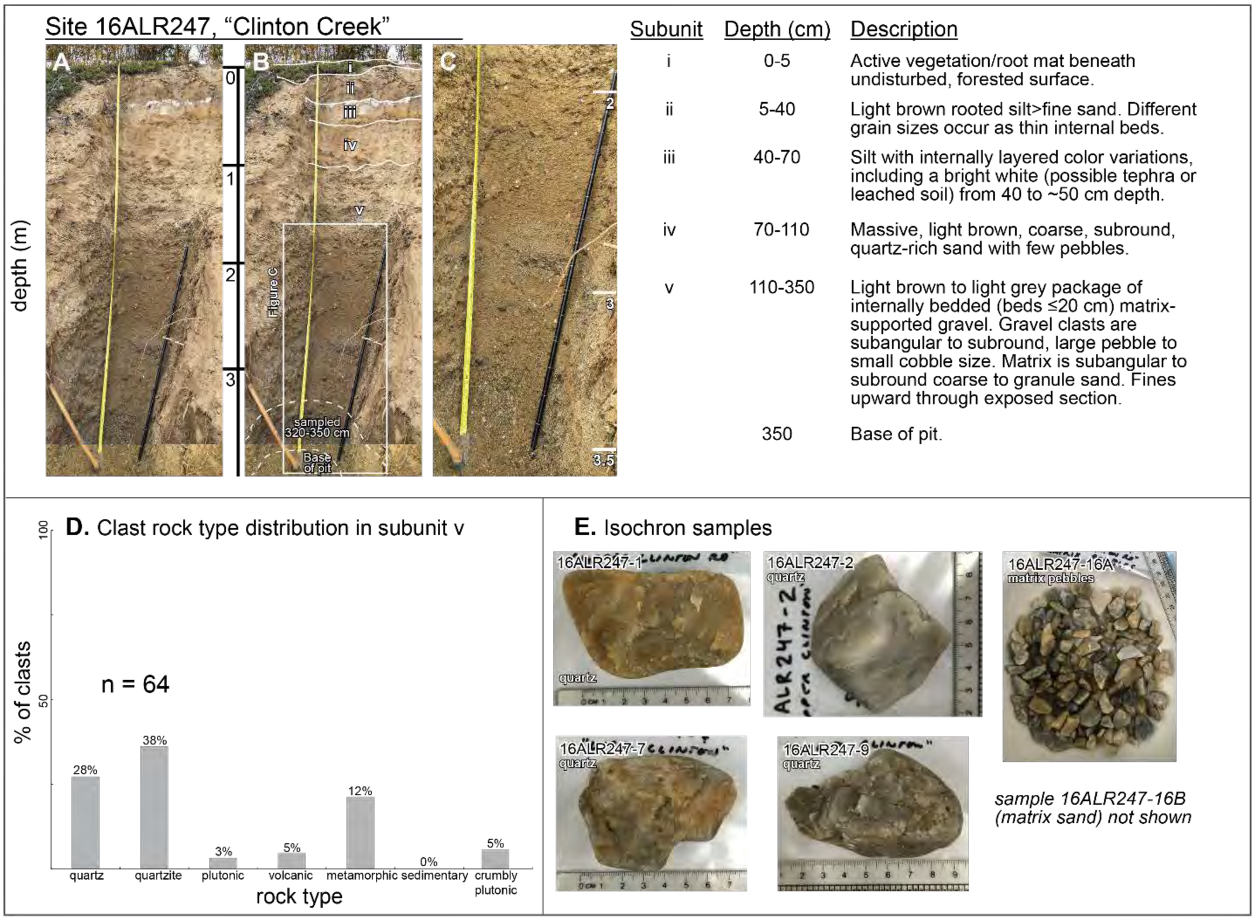

Figure DR1: Description for isochron burial age sample site 16ALR247, located in Yukon, Canada near the Fortymile-Yukon River confluence at NAD1983 UTM coordinates 64.37448, -140.59348. (A) Un-interpreted photo of sample pit. (B) Sample pit with stratigraphic interpretation of subunits. Solid white lines represent contacts, dashed white lines represent sampled interval, from 320 cm to the base of the pit at 350 cm. (C) Enlarged, un-interpreted photo of subunit v, which we sampled the bottom 30 cm of for cosmogenic isochron burial dating. (D) Rock type percentages from a count of 64 clasts in subunit v (110-350 cm depth). (E) Samples submitted for cosmogenic isochron burial age analysis (Tables DR1, DR2). Rock type for cobbles indicated in white text. Scale is shown in centimeters and varies between photos. Amalgamated matrix pebbles and sand (not shown) processed and treated as individual samples.

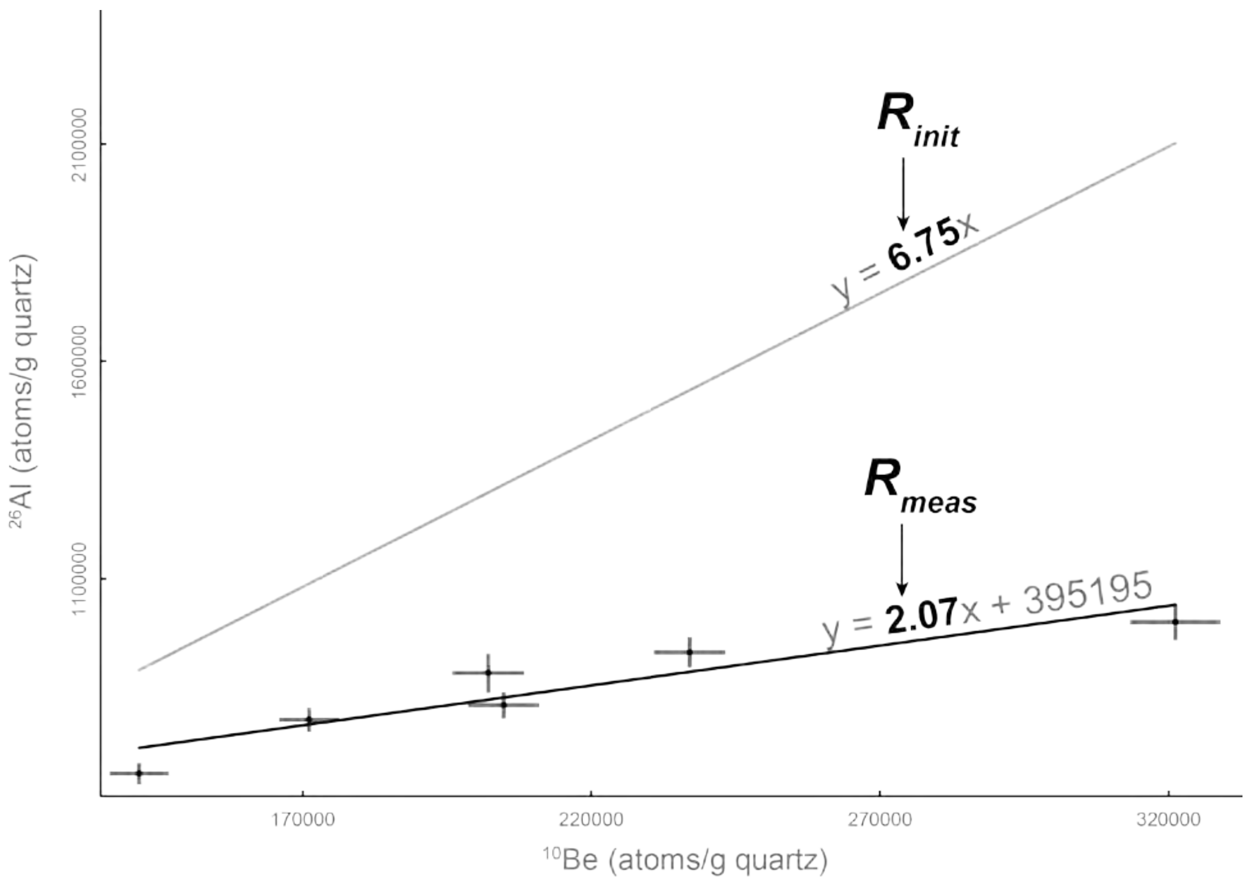

Figure DR2: Isochron plot with line fit to Clinton Creek data (slope provides R_{meas}) and line representing surface production ratio for the Clinton Creek samples (R_{init} assumed ~6.75).

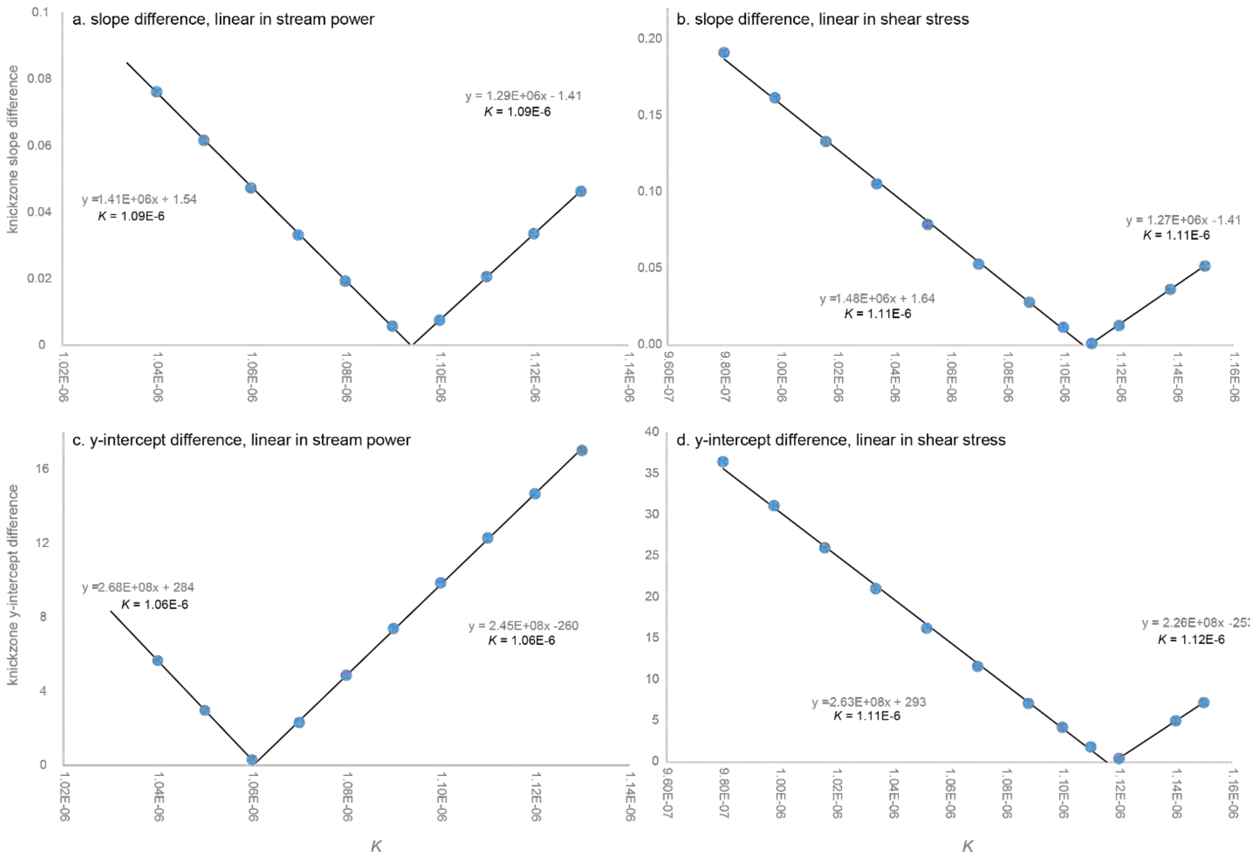

Figure DR3: Plots used to quantify a uniform Fortymile River *K* value from minimized linear regression statistic differences. (A) Difference in slope from modeled and DEM knickzone long profiles plotted over *K* value where $m = 0.6$ and $n = 1$ such that bedrock incision is linearly proportional to stream power, and (B) where $m = 0.4$ and $n = 0.67$ such that bedrock incision is linearly proportional to shear stress. (C) Difference in y-intercept from regressions of modeled and DEM knickzone long profiles plotted over *K* value where $m = 0.6$ and $n = 1$ such that bedrock incision is linearly proportional to stream power, and (D) where $m = 0.4$ and $n = 0.67$ such that bedrock incision is linearly proportional to shear stress.

REFERENCES CITED

Balco, G. and Rovey, C.W., 2008. An isochron method for cosmogenic-nuclide dating of buried soils and sediments. American Journal of Science, 308(10), pp.1083-1114.

Bender, A.M., Amos, C.B., Bierman, P., Rood, D.H., Staisch, L., Kelsey, H. and Sherrod, B., 2016. Differential uplift and incision of the Yakima River terraces, central Washington State. Journal of Geophysical Research: Solid Earth, 121(1), pp.365-384.

Bierman, P. and Steig, E.J., 1996. Estimating rates of denudation using cosmogenic isotope abundances in sediment. Earth surface processes and landforms, 21(2), pp.125-139.

Brown, E.T., Stallard, R.F., Larsen, M.C., Raisbeck, G.M., Yiou, F., 1995. Denudation rates determined from the accumulation of in situ-produced ^{10}Be in the luquillo experimental forest, Puerto Rico, Earth and Planetary Science Letters, v. 129, p.193-202, ISSN 0012-821X.

Chmeleff, J., von Blanckenburg, F., Kossert, K. and Jakob, D., 2010. Determination of the 10Be half-life by multicollector ICP-MS and liquid scintillation counting. Nuclear Instruments and Methods in Physics Research Section B: Beam Interactions with Materials and Atoms, 268(2), pp.192-199.

Corbett, L.B., Bierman, P.R., Rood, D.H., Caffee, M.W., Lifton, N.A. and Woodruff, T.E., 2017. Cosmogenic ^{26}Al/^{10}Be surface production ratio in Greenland. Geophysical Research Letters, 44(3), pp.1350-1359.

Foster, H.L., 1976, Geologic map of the Eagle quadrangle, Alaska: U.S. Geological Survey Miscellaneous Investigations Series Map 1–922, scale 1:250,000.

Finnegan, N.J., Schumer, R. and Finnegan, S., 2014. A signature of transience in bedrock river incision rates over timescales of 10^4–10^7 years. Nature, 505(7483), p.391.

Gallen, S.F., Pazzaglia, F.J., Wegmann, K.W., Pederson, J.L. and Gardner, T.W., 2015. The dynamic reference frame of rivers and apparent transience in incision rates. Geology, 43(7), pp.623-626.

Gosse, J.C. and Phillips, F.M., 2001. Terrestrial in situ cosmogenic nuclides: theory and application. Quaternary Science Reviews, 20(14), pp.1475-1560.

Granger, D.E., Kirchner, J.W. and Finkel, R., 1996. Spatially averaged long-term erosion rates measured from in situ-produced cosmogenic nuclides in alluvial sediment. The Journal of Geology, 104(3), pp.249-257.

Hancock, G.S. and Anderson, R.S., 2002. Numerical modeling of fluvial strath-terrace formation in response to oscillating climate. Geological Society of America Bulletin, 114(9), pp.1131-1142.

Hidy, A.J., Gosse, J.C., Froese, D.G., Bond, J.D. and Rood, D.H., 2013. A latest Pliocene age for the earliest and most extensive Cordilleran Ice Sheet in northwestern Canada. Quaternary Science Reviews, 61, pp.77-84.

Hidy, A.J., Gosse, J. C., Sanborn, P., Froese, D. G., 2018. Age-erosion constraints on an Early Pleistocene paleosol in Yukon, Canada, with profiles of ^{10}Be and ^{26}Al: Evidence for a significant loess cover effect on cosmogenic nuclide production rates, CATENA, v. 165, p. 260-271, ISSN 0341-8162, https://doi.org/10.1016/j.catena.2018.02.009.

Lal, D., 1991. Cosmic ray labeling of erosion surfaces: in situ nuclide production rates and erosion models. Earth and Planetary Science Letters, 104(2-4), pp.424-439.

Lague, D., 2014. The stream power river incision model: evidence, theory and beyond. Earth Surface Processes and Landforms, 39(1), pp.38-61.

Nishiizumi, K., 2004. Preparation of 26Al AMS standards. Nuclear Instruments and Methods in Physics Research Section B: Beam Interactions with Materials and Atoms, 223, pp.388-392.

Nishiizumi, K., Imamura, M., Caffee, M.W., Southon, J.R., Finkel, R.C., and McAninch, J., 2007, Absolute calibration of 10Be AMS standards: Nuclear Inst. and Methods in Physics Research, B, v. 258, no. 2, p. 403–413.

Schaller, M., Ehlers, T.A., Stor, T., Torrent, J., Lobato, L., Christl, M. and Vockenhuber, C., 2016. Timing of European fluvial terrace formation and incision rates constrained by cosmogenic nuclide dating. Earth and Planetary Science Letters, 451, pp.221-231.

Schildgen, T.F., Phillips, W.M. and Purves, R.S., 2005. Simulation of snow shielding corrections for cosmogenic nuclide surface exposure studies. Geomorphology, 64(1-2), pp.67-85.

Stock, J.D. and Montgomery, D.R., 1999. Geologic constraints on bedrock river incision using the stream power law. Journal of Geophysical Research: Solid Earth, 104(B3), pp.4983-4993.

Stone, J.O., 2000. Air pressure and cosmogenic isotope production. Journal of Geophysical Research: Solid Earth, 105(B10), pp.23753-23759.

Wobus, C., Whipple, K.X., Kirby, E., Snyder, N., Johnson, J., Spyropolou, K., Crosby, B., Sheehan, D., and Willett, S.D., 2006, Tectonics from topography: Procedures, promise, and pitfalls: Geological Society of America Special Paper, v. 398, p. 55, 10.1130/2006.2398(04).

Mahon, K.I., 1996. The New “York” regression: Application of an improved statistical method to geochemistry. International Geology Review, 38(4), pp.293-303.